The Investigation of Mechanical and Functional Properties and Microstructural Features of Coarse-Grained SME $Ti_{49.0}Ni_{51.0}$ Alloy during Multiple Martensitic Transformations and Annealing

Anna Churakova[1,2,*], *Elina* Kayumova[3], and *Dmitry* Gunderov[1,2]

[1]Institute of Molecule and Crystal Physics - Subdivision of the Ufa Federal Research Center of the Russian Academy of Sciences, 450075, 151 pr. Oktyabrya, Ufa, Russia
[2]Ufa State Aviation Technical University, 450008, 12 K. Marx str., Ufa, Russia
[3] Ufa State Petroleum Technological University, 450064, 1 Kosmonavtov st., Ufa, Russia

Abstract. The paper was investigated the effect of preliminary multiple martensitic transformations on the microstructure and mechanical and functional stability during subsequent annealing in the range of aging temperatures of the $Ti_{49.0}Ni_{51.0}$ alloy in the coarse-grained state. The structure in the initial state has an austenitic structure with a grain size of 35 ± 2 μm; after TC, the structure is martensite with a grain size of 30 ± 5 μm. According to the results of mechanical tensile tests, thermal cycling leads to an increase in the yield stress, which is associated with the generation and accumulation of dislocations. An increase in the number of cycles to n = 100 led to a slight decrease in the yield stress, which may be due to the saturation effect during thermal cycling. Subsequent aging at T=400 °C after thermal cycling showed that the yield stress increases. At the same time, the results of mechanical tests showed that, in general, the preliminary TC (n = 100) with subsequent aging contributes to an increase in the yield strength and strength. The structure revealed after thermal cycling and subsequent low-temperature annealing confirms the precipitation of aging strengthening particles Ti_3Ni_4.

1 Introduction

The NiTi shape memory alloys exhibit excellent characteristics such as shape memory effect and superelasticity and are promising materials for practical applications [1-3]. During operation, NiTi devices usually undergo a cyclic phase transformation between the austenite phase (A) and the B19' structure of martensite (M) [2]. The discrepancy between the volumes of the B2/B19' phases upon transformation leads to the generation of dislocations and plastic deformation [4–12]. Irreversible plastic deformation accumulates during cyclic phase transformation, leading to a decrease in functional properties

* Corresponding author: churakovaa_a@mail.ru

(functional fatigue) [6,8,13]. Thus, the prevention of plastic deformation by increasing the strength of the NiTi matrix is necessary to reduce the accumulation of irreversible plastic deformation and thus improves the functional stability of NiTi alloys. Among all existing methods of hardening metallic materials - grain refining and precipitation hardening, is widely considered as an effective method to improve the functional stability of NiTi alloys [14–18]. Various studies of the functional characteristics of ultrafine-grained NiTi alloys have shown that functional stability can be significantly improved upon grain refinement to about 100 nm [7,11,15,17–19], but the structure with such a grain size suppresses the martensitic transformation B19′ [20,21], leading to a change in the dependence of deformation on stress from superelastic to linear elasticity [19,22]. The most famous methods of obtaining NiTi alloys with nanostructure are methods of severe plastic deformation (for example, cold drawing [15], high pressure torsion [23], extrusion with an equal channel angle [24], repeated cold rolling [25]) followed by heat treatment [15,22]. With such processing, the main task is to keep the grain size in a certain range for high plasticity (deformation with elongation up to 50% [26]), high strength and high impact toughness inherent in NiTi alloys [27]. Isolation of aging particles of Ni_4Ti_3 is an alternative effective method for increasing the strength of the matrix and, accordingly, increasing the functional stability in alloys with a high nickel content [14, 16, 28, 29]. To isolate aging particles, heat treatment is required [1], which, in turn, also promotes grain growth (several tens of microns). A large grain size can lead to a nonuniform distribution of Ni_4Ti_3 particles both in the grain body and at the boundaries [30–34]. Such an inhomogeneous distribution of particles can also lead to a change in the nature of the martensitic transformation, for example, to multistage transformations [1,31–35]. In [16,30,36] works it was found that by controlling the grain size during aging, it is possible to influence the phase transformation and properties. Thus, low-temperature aging of NiTi alloys with relatively fine grains (for example, several microns [16,36]) promotes a more uniform distribution of Ni_4Ti_3 particles. A more interesting approach is to use as a technique of raising the yield stress multiple martensitic transformations (thermal cycling - TC) [37], which in turn will also contribute to a more uniform release particles during aging anneals to dislocation accumulated under them. This work is devoted to the study of this approach during aging both in the low-temperature region and in the field of classical aging.

2 Material and methods

Two-component alloy were selected as the research material the $Ti_{49.0}Ni_{51.0}$ alloy, at room temperature has the structure of B2 austenite. To form a solid solution based on TiNi the alloy was quenched from the homogeneity region (from 800 °C) into water. The average grain size of the hardened alloy was 50 μm. Thermal cycling of the samples in different initial states was carried out as follows: the samples were successively immersed in liquid nitrogen (−196 °C), then they were heated to a temperature of 150 °C, which is actually lower and higher than the temperatures M_f of direct and A_f reverse martensitic transformation. The number of heating – cooling thermal cycles ranged from 0 to 100 [22-23]. The fine structure of the material was studied at room temperature using a JEOL JEM-2100 transmission microscope with an accelerating voltage of 200 kV. Samples for thin foils cut by the electro-polishing method were made by double-sided jet electrolytic polishing using a Tenupol-5 device in a solution of 10% perchloric acid and 90% butanol. Mechanical tensile tests were carried out on small specimens at a tensile rate of 0.24 mm/min. Fractography was researched using a scanning electron microscope JEOL JSM 6390.

3 Results

After quenching, the structure of the coarse-grained (CG) $Ti_{49.0}Ni_{51.0}$ alloy is austenite, which is represented by equiaxed grains with a size of 35 ± 2 μm (Figure 1, a), and aging at T = 400 ℃ leads to a change in the grain size to 30 ± 2 μm (Figure 1, b).

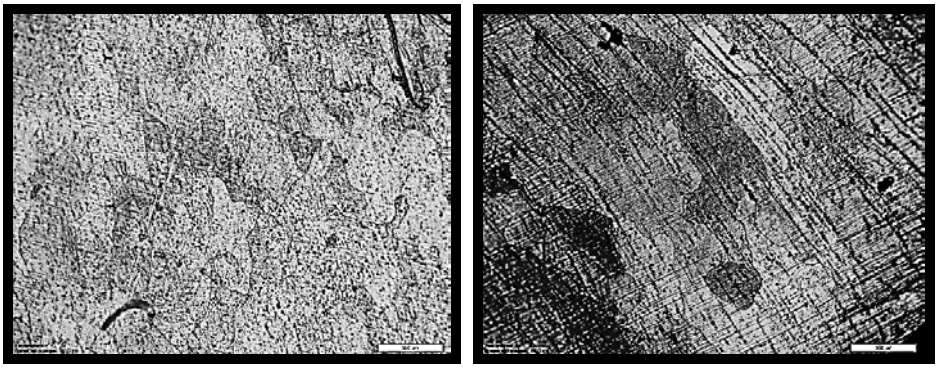

a b

Fig. 1. The structure of the $Ti_{49.0}Ni_{51.0}$ alloy in the CG state: a) initial state, b) aging T = 400 ℃

After TC n = 20, the structure of the coarse-grained $Ti_{49.0}Ni_{51.0}$ alloy had an austenitic structure with a grain size of 30 ± 2 μm, (Figure 2, a), TC n = 100 leads to a decrease in the grain size to 25 ± 2 μm, in some area's martensite plates (Figure 2, b).

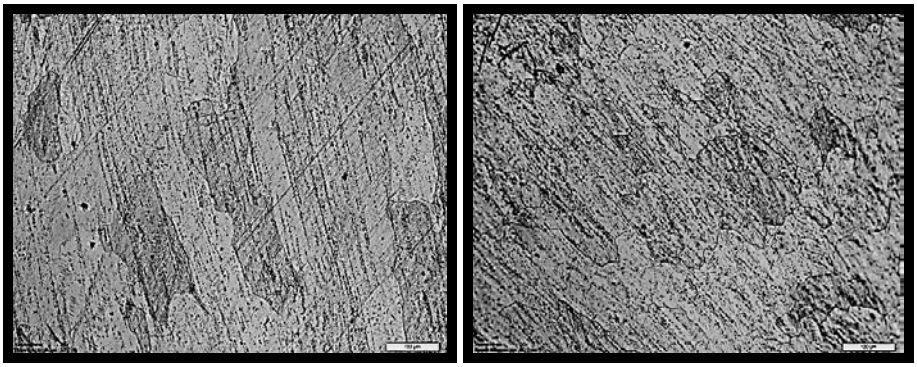

a b

Fig. 2. The structure of the $Ti_{49.0}Ni_{51.0}$ alloy in the course-grained state: a) n = 20 cycles, b) n = 100 cycles

After TC n = 20 T = 400 ℃, the structure of the coarse-grained $Ti_{49.0}Ni_{51.0}$ alloy had a grain size of 30 ± 2 μm (Figure 3, a), at n = 100 T = 400 ℃, the grain size is 25 ± 2 μm, grain boundaries are clearly visible (Figure 3, b).

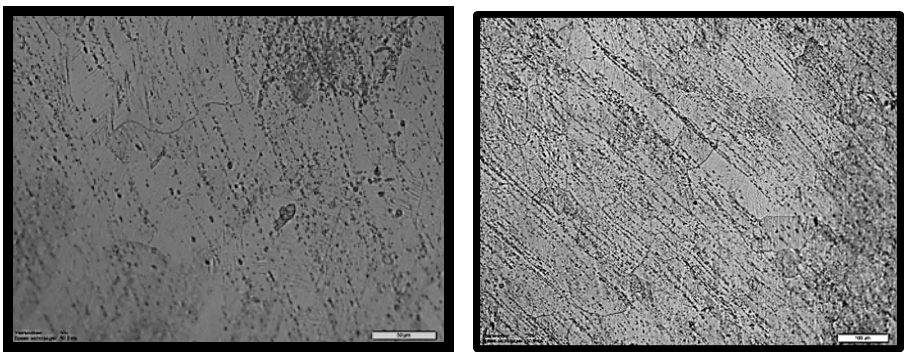

a b

Fig. 3. The structure of the $Ti_{49.0}Ni_{51.0}$ alloy in the CG state: a) n = 20 and annealing at 400 °C, b) n = 100 and annealing at 400 °C

However, it is not possible to study the fine structure by optical metallography; for this, transmission electron microscopy was used.

In the initial state, the structure is represented by practically pure dislocation-free grains of B2 austenite (Figure 4, a, b). Aging at a temperature of 400 °C of the initial state leads to changes in the structure - aging particles are released both in the body of the grains and at the boundaries (Figure 4, c, d).

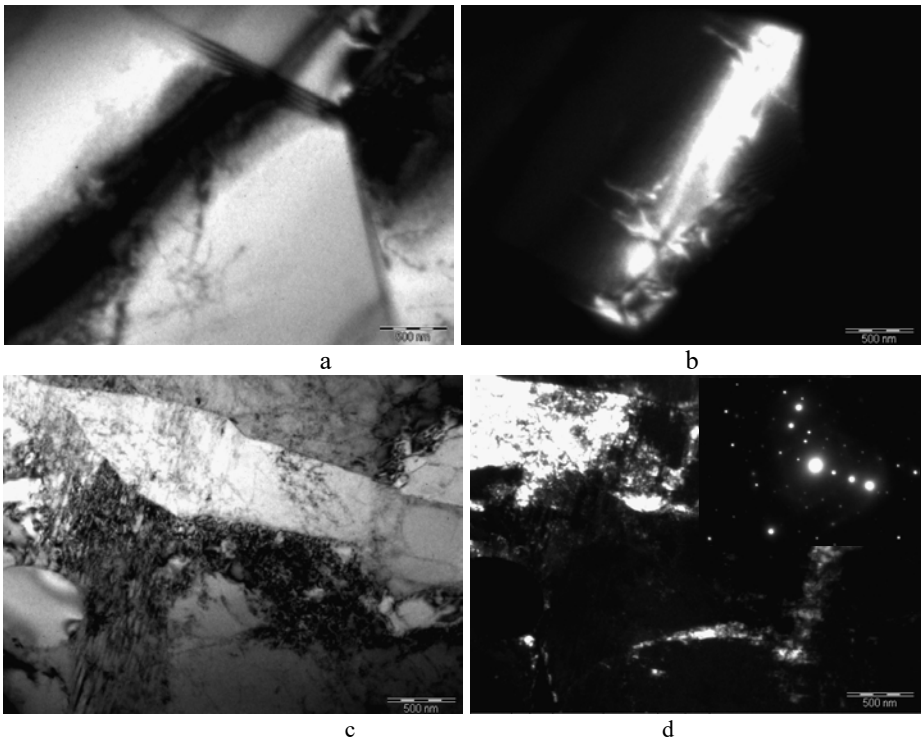

a b

c d

Fig. 4. The structure of the $Ti_{49.0}Ni_{51.0}$ alloy in the CG state: a) the initial state, b) aging T = 400 °C

Thermal cycling with the maximum number of cycles leads to a noticeable and significant accumulation of dislocations in the grain body (Figure 5).

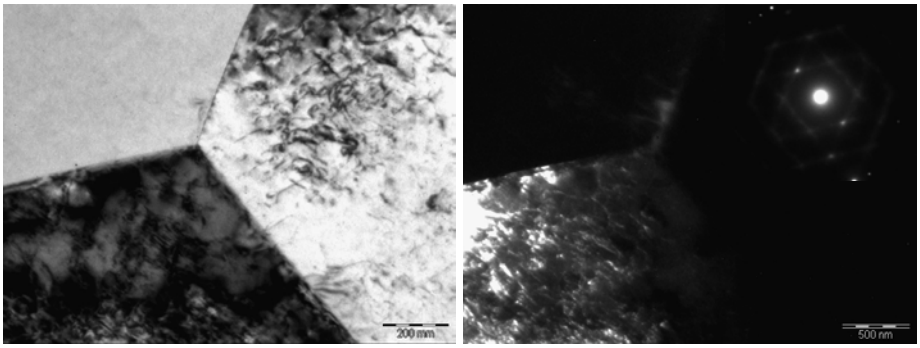

Fig. 5. The structure of the $Ti_{49.0}Ni_{51.0}$ alloy in the CG state and thermal cycling n = 100 cycles

Annealing at an aging temperature of 400 °C after thermal cycling with the maximum number of cycles leads to the precipitation of aging particles predominantly on dislocation networks in the grain body (Figure 6). In this case, the density of dislocations decreases somewhat.

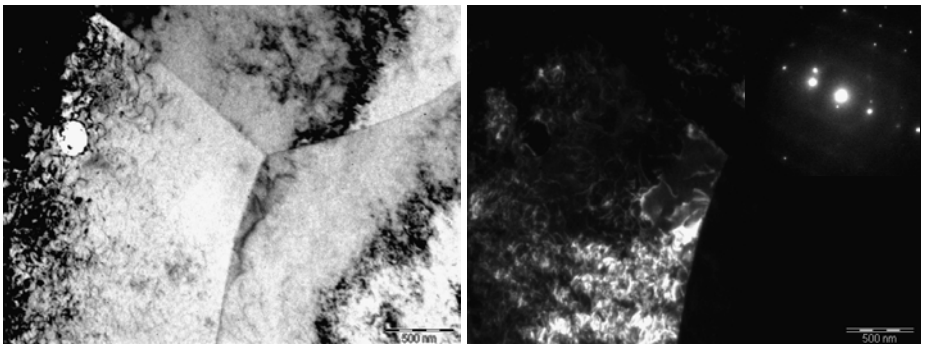

Fig. 6. The structure of the $Ti_{49.0}Ni_{51.0}$ alloy in the CG state, thermal cycling n = 100 and annealing at 400 °C

Also, studies were carried out and low-temperature aging at a temperature of 250 °C after the maximum number of cycles (Figure 7). In this state, the approach with the separation of aging particles on dislocation networks formed during multiple martensitic transformations is also confirmed.

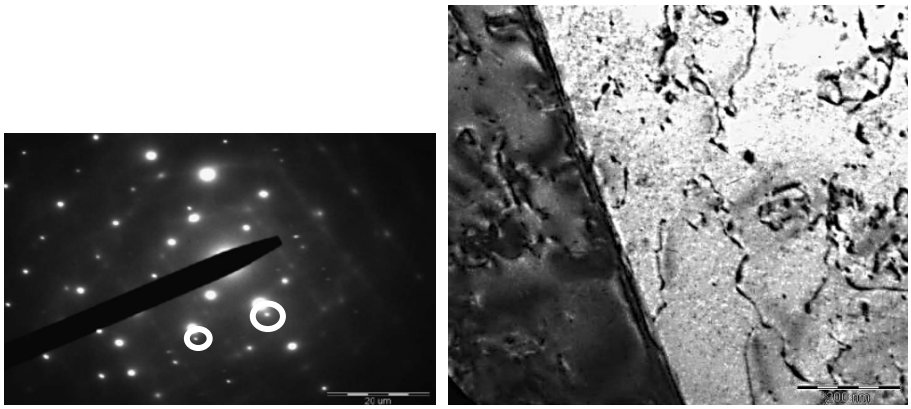

a b

Fig. 7. Typical TEM images of the structure: a) electron diffraction pattern, b) bright-field image

Mechanical tests were carried out on samples of the $Ti_{49.0}Ni_{51.0}$ alloy in the CG state before and after TC, followed by aging in the temperature range 250-400 °C. For each condition, 3 samples were tested. The results of mechanical tests are presented in table 1.

In the quenched state, the alloy had a tensile strength of 1045 MPa, however, aging at 400 °C lowers its strength to 910 MPa, the phase yield strength and plasticity also decrease from 33 to 24%, and the dislocation yield strength increases. TC n = 20 in the quenched state leads to an increase in the yield stress from 460 MPa to 665 MPa as compared to SC to TC, which is associated with the generation and accumulation of dislocations. An increase in the number of cycles to n = 100 led to a slight decrease in the yield stress, which may be due to the saturation effect at TC. Subsequent aging at T = 400 °C after TC showed that the yield point increases to 690 MPa, which is associated with a more uniform distribution of aging particles on dislocation networks. With subsequent aging at a temperature of 400 °C, the level of properties is retained, which also confirms the idea of increasing functional stability.

Table 1. Results of mechanical tensile tests

State		σ_{UTS}, MPa	σ_m, MPa	σ_{YS}, MPa	σ_{reac}, MPa	δ, %
CG	Initial	1045±30	255±15	460±20	205±15	33±5
	Annealing 250°C	935±30	225±15	570±25	345±15	25±5
	Annealing 400°C	910±30	225±15	595±20	370±15	24±5
	TC n=20	1020±20	345±15	665±20	320±15	18±5
	TC n=100	985±30	330±15	635±20	305±15	20±5
	TC n=20 + Annealing 250°C	895±25	340±15	660±20	320±10	20±5
	TC n=100 + Annealing 250°C	1100±30	352±15	670±20	320±10	24±5
	TC n=20 + Annealing 400°C	980±20	205±15	690±20	485±10	20±5
	TC n=100 + Annealing 400°C	935±25	215±15	670±20	355±15	18±5

The fracture of the $Ti_{49.0}Ni_{51.0}$ alloy in Figure 8, a has a shallow character with a pits size of 13 ± 2 μm in the initial state during quenching, the nature of the fracture is brittle. With aging at 250 and 400 °C, in some areas, aging particles are observed at the tops of the pits, the pits have a size of 18 ± 2, 15 ± 2 μm, respectively, the destruction is brittle, oxide particles are partially present (b, c).

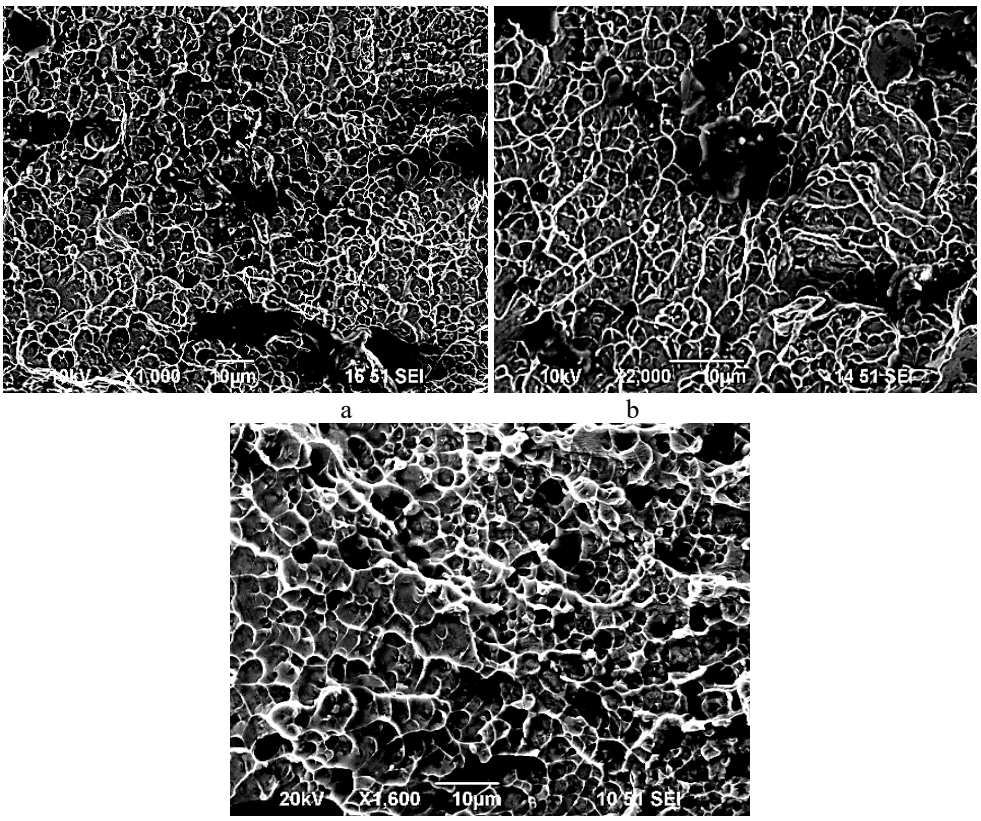

a b c

Fig. 8. The fracture structure of $Ti_{49.0}Ni_{51.0}$ in the initial SC state: a) quenching at 800 °C, b) aging at 250 °C, c) aging at 400 °C

In Figure 9 the fracture in the TC state n = 100 was of brittle nature, the pits are oblong with a size of 15 ± 2 μm. Figure 9b shows the fracture after TC n = 100 T = 400 °C had brittle ductile.

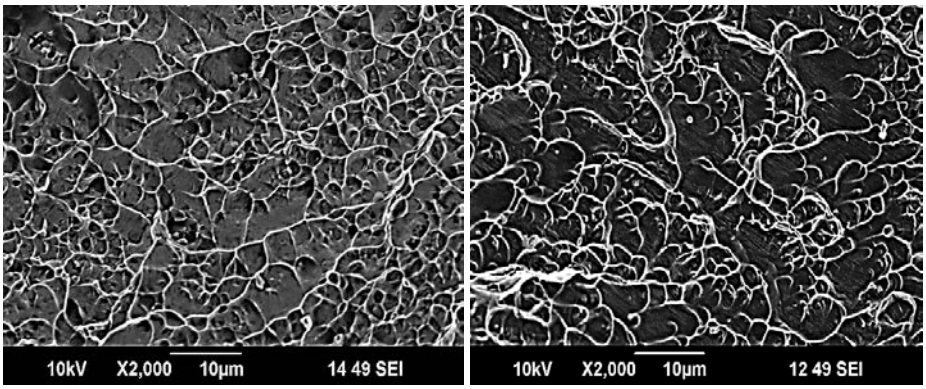

a b

Fig. 9. Structure of fracture $Ti_{49.0}Ni_{51.0}$ in CG + TC n = 100 (a), n = 100 T = 400 °C (b)

4 Conclusion

The structure in the initial CG state has an austenite structure with a grain size of 35 ± 2 μm; after TC the structure is martensite with a grain size of 30 ± 5 μm. According to the results of mechanical tensile tests, CG + TC n = 20 leads to an increase in the yield stress, which is associated with the generation and accumulation of dislocations. An increase in the number of cycles to n = 100 led to a slight decrease in the yield stress, which may be due to the saturation effect at TC. Subsequent aging at T = 400 °C after TC n = 20 showed that the yield stress increases, which can be explained by the distribution of aging particles on dislocation networks formed during TC. A significant decrease at n = 100 can be associated with a high density of defects and aging particles, which lead to the destruction of samples at lower values of the ultimate strength, hindering the movement of dislocations.

Analysis of fractography shows that in the $Ti_{49.0}Ni_{51.0}$ alloy in the CG state, a shallow fracture is expressed with a pit size of 13 ± 2 μm, in which there are characteristic inclusions of aging particles, brittle fracture prevails, however, in the same alloy, but with TC the nature of the fracture becomes quasi-brittle, that is, it combines brittle-ductile fracture and has an elongated pits shape.

The authors acknowledge gratefully the financial support of the research provided by the Russian Science Foundation through project № 20-72-00075.

References

1. K. Otsuka, X. Ren, Prog. Mater. Sci., **50** (2005).
2. K. Yamauchi, I. Ohkata, K. Tsuchiya, S.Miyazaki, *ShapeMemory and Superelastic Alloys:Technologies and Applications*, (Woodhead Publishing, Cambridge, UK, 2011).
3. L. Lecce, A. Concilio, *Shape Memory Alloy Engineering for Aerospace, Structural and Biomedical Applications*, (Butterworth-Heinemann, Oxford, UK, 2015).
4. J. Zhang, C. Somsen, T. Simon, X. Ding, S. Hou, S. Ren, X. Ren, G. Eggeler, K. Otsuka, J. Sun, Acta Mater. **60** (2012).
5. M.L. Bowers, X. Chen, M. De Graef, P.M. Anderson, M.J. Mills, Scr. Mater. **78-79** (2014).
6. P. Chowdhury, H. Sehitoglu, Prog. Mater. Sci. **85** (2017).
7. R. Delville, B. Malard, J. Pilch, P. Sittner, D. Schryvers, Int. J. Plast. **27** (2011).
8. Y. Gao, L. Casalena, M.L. Bowers, R.D. Noebe, M.J. Mills, Y. Wang, Acta Mater. **126** (2017).
9. H.M. Paranjape, M.L. Bowers, M.J. Mills, P.M. Anderson, Acta Mater. **132** (2017).
10. A.W. Richards, R.A. Lebensohn, K. Bhattacharya, Acta Mater. **61** (2013).
11. P. Sedmak, P. Sittner, J. Pilch, C. Curfs, Acta Mater. **94** (2015).
12. T. Simon, A. Kröger, C. Somsen, A. Dlouhy, G. Eggeler, Acta Mater. **58** (2010).
13. 13. G. Eggeler, E. Hornbogen, A. Yawny, A. Heckmann,M.Wagner, Mater. Sci. Eng. A **378** (2004).
14. J.I. Kim, S. Miyazaki, Acta Mater. **53** (2005).
15. R. Delville, B. Malard, J. Pilch, P. Sittner, D. Schryvers, Acta Mater. **58** (2010).
16. X. Wang, S. Kustov, K. Li, D. Schryvers, B. Verlinden, J. Van Humbeeck, Acta Mater. **82** (2015).

17. A. Ahadi, Q. Sun, Acta Mater. **90** (2015).
18. A. Yawny, M. Sade, G. Eggeler, Z. Metallkd. **96** (2005).
19. B. Malard, J. Pilch, P. Sittner, V. Gartnerova, R. Delville, D. Schryvers, C. Curfs, Funct. Mater. Lett. **2** (2009).
20. T. Waitz, K. Tsuchiya, T. Antretter, F.D. Fischer, MRS Bull. **34** (2009).
21. T. Waitz, V. Kazykhanov, H.P. Karnthaler, Acta Mater. **52** (2004).
22. A. Ahadi, Q. Sun, Acta Mater. **76** (2014).
23. M. Peterlechner, T. Waitz, H.P. Karnthaler, Scr. Mater. **60** (2009).
24. B. Kockar, I. Karaman, J.I. Kim, Y. Chumlyakov, J. Sharp, C.-J. Yu, Acta Mater. **56** (2008).
25. M. Peterlechner, J. Bokeloh, G. Wilde, T. Waitz, Acta Mater. **58** (2010).
26. S. Miyazaki, Y. Kohiyama, K. Otsuka, T.W. Duerig, Mater. Sci. Forum **765** (1990).
27. M. Elahinia, N.S. Moghaddam, M.T. Andani, A. Amerinatanzi, B.A. Bimber, R.F. Hamilton, Prog. Mater. Sci. **83** (2016).
28. H.E. Karaca, S.M. Saghaian, G. Ded, H. Tobe, B. Basaran, H.J. Maier, R.D. Noebe, Y. Chumlyakov, Acta Mater. **61** (2013).
29. S. Miyazaki, T. Imai, Y. Igo, K. Otsuka, Metall. Trans. A. **17** (1986).
30. X. Wang, C. Li, B. Verlinden, J. Van Humbeeck, Scr. Mater. **69** (2013).
31. X. Wang, B. Verlinden, S. Kustov, Funct. Mater. Lett. **10** (2017).
32. B. Karbakhsh Ravari, S. Farjami, M. Nishida, Acta Mater. **69** (2014).
33. Y. Zhou, J. Zhang, G. Fan, X. Ding, J. Sun, X. Ren, K. Otsuka, Acta Mater. **53** (2005).
34. J. Khalil-Allafi, A. Dlouhy, G. Eggeler, Acta Mater. **50** (2002).
35. J.I. Kim, Y. Liu, S. Miyazaki, Acta Mater. **52** (2004).
36. X.Wang, K. Li, D. Schryvers, B. Verlinden, J. Van Humbeeck, Scr. Mater. **72-73** (2014).
37. A.A Churakova, D.V. Gunderov, Acta Metallurgica Sinica (English Letters) **28** (2015).